Supporting information for : The role of cell-mediated enzymatic degradation and cytoskeletal tension on dynamic changes in the rheology of the pericellular region prior to human mesenchymal stem cell motility

Maryam Daviran, Hugo S. Caram, and Kelly M. Schultz*

Department of Chemical and Biomolecular Engineering, Lehigh University, Bethlehem, PA 18015

E-mail: kes513@lehigh.edu

Phone: (610) 758-2012. Fax: (610) 758-5057

Supporting figures S1-S10

Number of pages: 19

Materials

3mM of 4-arm star poly(ethylene glycol) (PEG) functionalized with norbornene (7.2×10^{18} -ene groups, -ene functionality= 4, Sigma-Aldrich, Saint Louis, MO) is chemically cross-linked with 3.9 mM of a matrix metalloproteinase (MMP) degradable peptide sequence, KCGPQG↓IWGQCK (4.7×10^{17} thiol groups, thiol functionality= 2, MW=1304.6 g mol^{-1}, peptide purity: 90.6%, water solubility: 1 mg mL^{-1}, peptide content: 88.8%, counter ion: Chloride, appearance: white lyophilized powder, American Peptide, Inc., Sunnyvale, CA).[1] Other components of the gel include 1 mM of an adhesion ligand, CRGDS (thiol functionality= 1, American Peptide, Inc., Sunnyvale, CA), 2×10^5 cells mL^{-1} of human mesenchymal stem cells (hMSCs), 1.7 mM of lithium phenyl-2,4,6-trimethylbenzoylphosphinate (LAP is synthesized in the Anseth group using the previously described protocol[2]) and 0.1% solids per volume carboxylated polystyrene probe particles ($2a = 1 \pm 0.02$ μm, where a is particle radius, Polysciences, Inc., Warrington, PA). All the components are used as received and diluted in 1× phosphate buffered saline (1× PBS, Life Tech, Carlsbad, CA). The total volume of each hydrogel is 17μL.

Cell culture and treatment with inhibitors

hMSCs are obtained from Lonza (Walkersville, MD). They are cultured in growth media which contains low-glucose Dulbecco's modified Eagle's medium (DMEM, Life Technologies, Carlsbad, CA), 10% Fetal Bovine Serum (FBS, Life Technologies, Carlsbad, CA), 1 ng mL^{-1} recombinant human fibroblast growth factor (hFGF, Peprotech, Rocky Hill, NJ), 0.5 μg mL^{-1} Fungizone (Life Technologies, Carlsbad, CA) and 50 U mL^{-1} Penicillin/streptomycin (Life Technologies, Carlsbad, CA). Cells are kept in the incubator at 5% CO_2 and 37°C. Passages 2−5 are used for experiments.

To inhibit myosin II (cytoskeletal tension), 2 hours after encapsulation cells are treated with 50 μM blebbistatin, a myosin II inhibitor, (Sigma-Aldrich, Saint Louis, MO) and incubated

overnight at 37°C and 5% CO_2.[3] To inhibit MMPs, cells are immediately treated with 10μM InSolution GM 6001 (MMP inhibitor) (Millipore Sigma, Darmstadt, Germany) after encapsulation.

We measure cells isolated from several different donors across these experiments. For untreated cells, hMSCs are from three different donors and we measure no changes in cell-mediated degradation. The blebbistatin and MMP inhibition hMSCs are from a single donor. For each condition that is measured, we use three biological replicates and for each biological replicate there are at least two hydrogels made. This ensures that there is no biological dependence or hydrogel dependence in the data. Through all these conditions tested, we do not measure changes in cell-mediated degradation profiles.

Device fabrication and cell encapsulation

A sample chamber is fabricated out of a glass-bottomed petri dish (D = 0.35 mm, MatTek Corporation, Ashland, MA) and polydimethylsiloxane (PDMS, Dow Corning, Midland, MI) tubes to enable multiple particle tracking microrheology measurements of cell-laden hydrogels. Briefly, PDMS sheets are made by mixing the silicone elastomer base with the cross-linking agent at a ratio of 10:1 and curing at 65°C overnight. Then, a tube of PDMS is cut from the sheet using biopsy punches with an outer diameter of 10 mm and an inner diameter of 6 mm. PDMS chambers are attached to the glass bottom of the petri dishes using small amounts of uncured PDMS. To enable attachment to the petri dish, dishes are heated in the oven to 65°C and left overnight. These chambers are used to reduce probe particle drift during matrix degradation measurements.[1,4]

Petri dishes are sterilized with 70% ethanol. Gel precursor solutions are loaded into the PDMS sample chambers in the petri dishes. The gel precursor solution is photopolymerized by exposure to ultraviolet light for 3 minutes (365 nm light, 10 mW cm^{-2}, UVP, LLC, Upland, CA). Petri dishes are then filled with 4 mL of growth media (without hFGF) to

maintain high cell viability. Samples are incubated for $18-24$ hours before microrheological measurements are taken to allow cells to relax and begin to migrate.

Multiple particle tracking microrheology

Multiple particle tracking microrheology (MPT) characterizes the dynamic hydrogel properties during cell-mediated degradation and motility. MPT is a passive microrheological technique that measures the movement of fluorescently labeled probe particles embedded in the scaffold.[5,6] For untreated cell experiments, data are taken on an inverted microscope (Observer Z1, Carl Zeiss AG, Oberkochen, Germany) with a 63× water immersion objective (N.A. 1.3, 1× optovar, Carl Zeiss AG, Oberkochen, Germany). Videos are captured at 30 frames s^{-1} for 800 frames with an exposure time of 1000 μs (1024×1024 pixels, Miro M120, Vision research Inc., Wayne, NJ). These parameters minimize static and dynamic particle tracking errors in the data.[7] For cells treated with blebbistatin and the MMP inhibitor, data are collected using an inverted microscope (Nikon TE2000E, Nikon Instruments Inc., Melville, NY) using a 60× oil immersion objective (N. A. 1.4, 1× optovar, Nikon Instruments Inc., Melville, NY). Video microscopy captures probe particle movement at 30 frames s^{-1} for 800 frames with an exposure time of 1000 μs (CMOS high-speed camera, Hi-Spec 3, 1024×1280 pixels, Fastec Imaging Corp., San Diego, CA). Both microscopes have a cell incubation chamber that maintains samples at 37°C and 5% CO_2 during data collection to ensure cell viability and normal function.

Immediately before taking MPT data, a brightfield microscopy image of the same field of view is taken to determine the cell position. The position of the cell center is determined for each time point throughout data collection. For each cell, data are taken in the pericellular region every $5-6$ minutes over approximately one hour. The selection of the cells is arbitrary and is based on the shape of the cell. After encapsulation, cells have a rounded morphology but when they begin to migrate they attach to the network and stretch, which occurs imme-

diately before migration. Data are collected around both rounded and stretched cells and we determine that rounded cells do not degrade the pericellular region during the measurement time window (∼60 mins limited by photobleaching of probe particles). Stretched cells do degrade the scaffold past the gel-sol transition and motile cells are in a liquid environment on the probe particle measurement length scale (1 μm).

Control experiments

Two sets of control experiments are performed. First, hydrogels are made without hMSCs and incubated in media at the same condition. Data are taken over 2 days in 2 different hydrogels at 4-5 different areas. This data acquisition is repeated three times for a total of at least six hydrogels. Figure S1 shows the MPT measurements of the material over time for 5 different areas in one hydrogel. No scaffold degradation is measured.

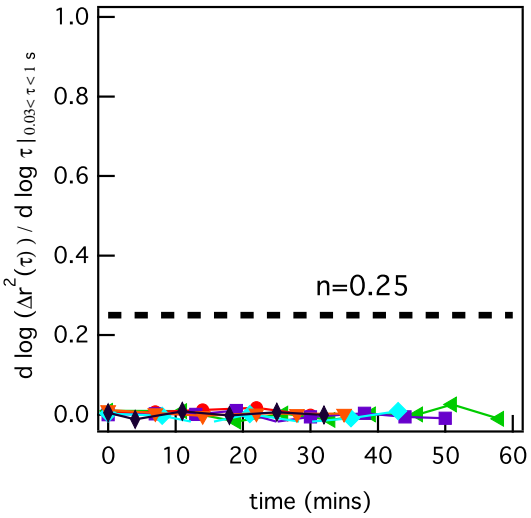

Figure S1: Changes in state of the material over 50 minutes for different areas in a hydrogel without cells.

Second, before cell-encapsulation experiments, hydrogels are made without cells and degraded in collagenase solutions to determine the rheological properties during degradation. This is a replicate of previously published data by Schultz et al.[4] Collagenase is a mixture

of enzymes, mostly MMPs, that degrade the MMP-degradable peptide cross-linker in this hydrogel scaffold. The hydrogel is degraded with different concentrations of collagenase, 2 mg/mL and 3 mg/mL. Figure S2 shows the data for a PEG-norbornene hydrogel incubated in 3 mg/mL of collagenase over time. Similar data is measured at 2 mg/mL over a longer time period. In Figure S2a, the material begins in the gel phase ($\alpha = 0$) and as time passes and collagenase degrades the cross-linkers and we measure an increase in the magnitude and logarithmic slope of the mean-squared displacement. This indicates that there is an increase in probe particle movement, indicative of larger pores and less scaffold structure. The change in magnitude also indicates an increase in the viscous component of the moduli and a decrease in the elastic component. After 1 hr the scaffold structure has degraded and probe particles are freely diffusing in a polymeric solution ($\alpha = 1$). Figure S2b, shows the logarithmic slope of the mean-squared displacement of the probe particle throughout time.

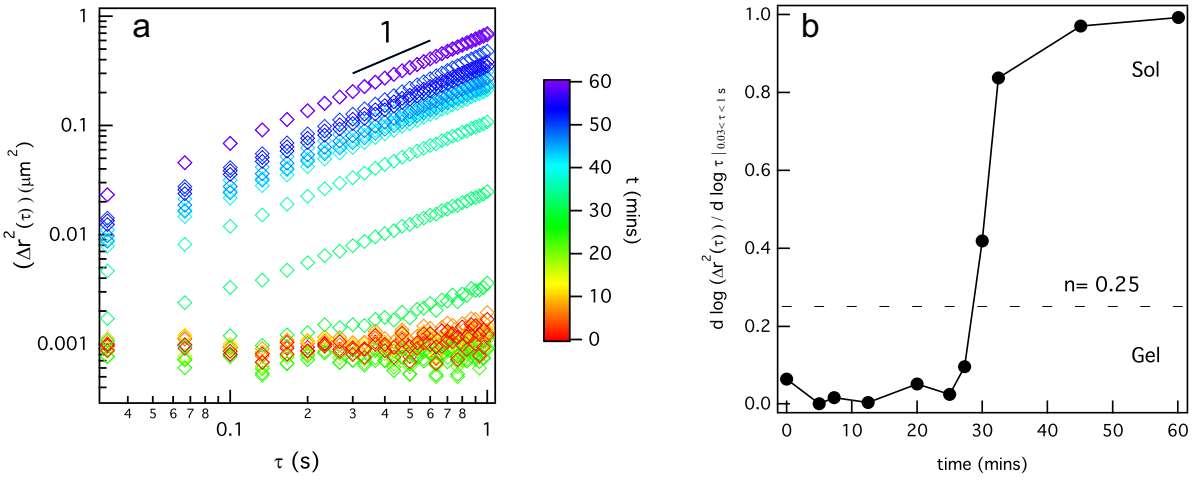

Figure S2: Measured mean-squared displacements for the degradation reaction of a PEG-norbornene hydrogel (0.65 thiol:ene) throughout time using 3 mg/ml of collagenase solution. a) Changes in the mean-squared displacements over time and b) the corresponding logarithmic slope of mean-squared displacement.

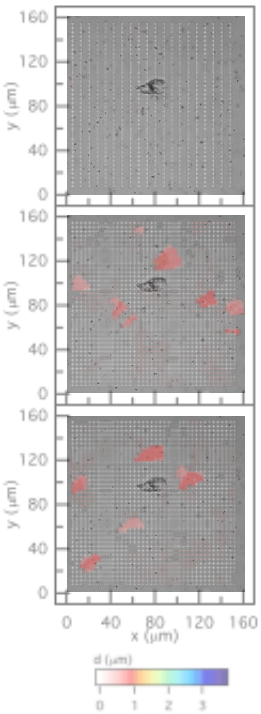

Figure S3: Spatial degradation profiles around an encapsulated hMSC prior to motility characterized using particle image velocimetry (PIV). Particle movement is determined from two brightfield images between (d) 0−6, (e) 30−36 and (f) 54−60 minutes using PIV. This movement is represented by colored vectors that show the magnitude and direction of each particles movement over this time period. The image of the cell is in the background.

Modified figures of degradation profiles around an encapsulated hMSC

Figure S3 shows the PIV data in figure 2 in the main text with the brightfield image of the cell in the background. Initially, we measure no probe particle displacement, which is quantified by the absence of velocity vectors, represented on the graph as white dots. In the middle image (t =30−36 mins), there is some particle displacement (represented by the color and size of the arrows) near the cell that is caused by cytoskeletal tension on the network. This displacement is very small, on the order of 1 μm, and is shown by PIV measurements around the cell and is in the same direction as the cell protrusion and subsequent cytoskeletal tension. Additionally, at the edge of the field of view we also measure some particle displacement, which is due to distortion of particles imaged at the edge of the field of view. Similarly, in the bottom image (t =54−60 mins), particle displacements around the cell are caused by

cytoskeletal tension on the network. Again, movement of particles at the edge of the field of view is a measurement artifact.

Due to the use of different experimental setups, we have cut the field of view in Figure 3 in the main text. This was done to make Figures 2 and 3 comparable in size. For blebbistatin treated cells, this data was collected on an experimental setup that had a wider field of view, the extended field of view for this degradation profile is shown in Figure S4.

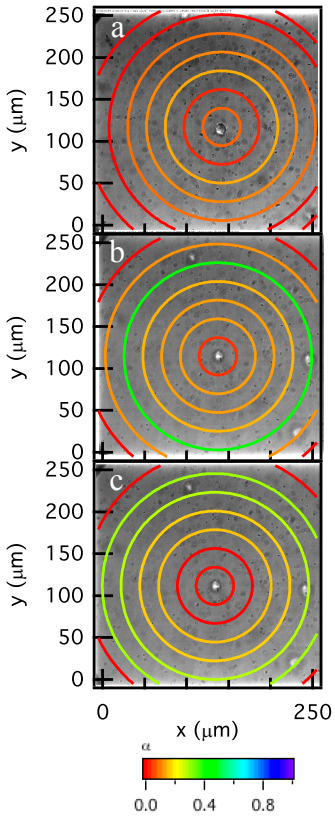

Figure S4: Spatial degradation profile around an encapsulated hMSC treated with a myosin II inhibitor prior to motility. MPT data are collected through time after identification of the hMSC at (a) 0, (b) 24 and (c) 35 minutes. The colored rings represent the logarithmic slope of the MSD, $\alpha = \frac{d\log\langle\Delta r^2(\tau)\rangle}{d\log\tau}$. This is the same degradation profile presented in Figure 3 in the text, but with an extended field of view. The field of view in Figure 3 in the text was limited to match the field of view of the untreated hMSC in Figure 2.

Additional degradation profiles around encapsulated hMSCs

Data are taken around encapsulated cells for acquisition windows between 30−60 mins. The total time of data acquisition around a single cell varies due to the cell speed and photobleaching of probe particles. The time between data points is limited by the experimental setup, namely the time to save acquired movies (2−3 mins). To maximize the total time of data acquisition samples are collected every 5−6 minutes. Compact spatial maps in the main text highlight the changes in the rheological properties in the pericellular region. The different treatment of cells (i.e. untreated, MMP inhibited and myosin II inhibited) have different time scales of scaffold degradation. For cells prior to migration, data collection is spaced out to take a longer absolute time of data, usually around 60 minutes. When a cell is moving, data is acquired more rapidly, usually limiting the absolute time of data acquisition to between 30−45 minutes. Figure S5a-h is the complete degradation profile for the untreated cell presented in the main text in Figure 2. Throughout the 60 minutes of data acquisition, we measure the transition in the pericellular region from a gel to a sol. Additionally, throughout cell-mediated degradation, the degradation profile measures the highest cross-link density directly around the cell while the cross-link density decreases as the distance from the cell center increases.

Figure S6a-c is a degradation profile for an hMSC where degradation occurs much quicker, 26 mins after data acquisition is begun. Although this scaffold degradation happens over a shorter time scale than that in Figure S5, the spatial changes in the rheology of the pericellular region are the same. The right column of Figure S6d-f shows particle image velocimetry (PIV) data with the hMSC is outlined. Large arrows near the cell center in Figure S6d show cytoskeletal tension created by the cell. Figure S6e and f show that particle movement is largest in the region furthest from the cell center, agreeing with MPT data.

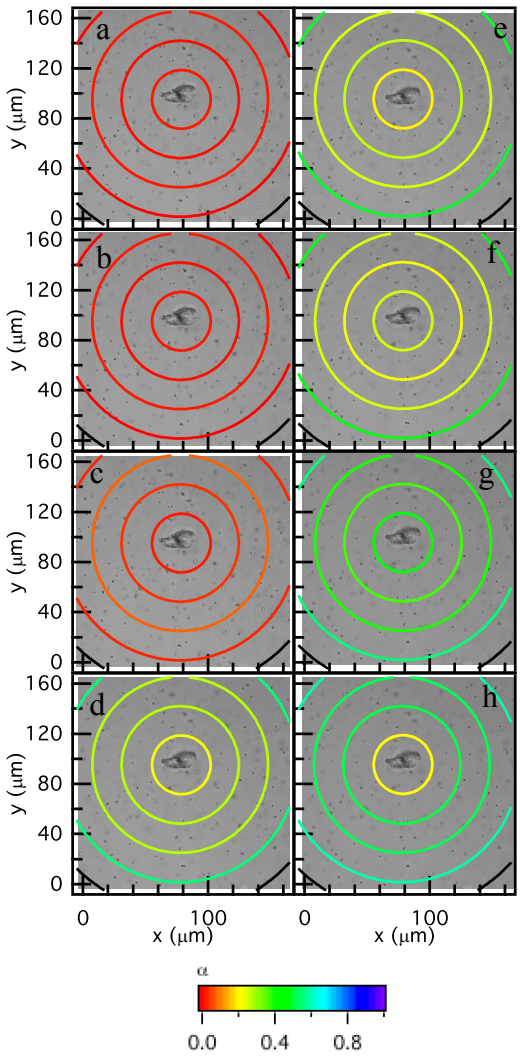

Figure S5: Spatial degradation profiles around an encapsulated hMSC prior to motility. MPT data are collected through time after identification of the hMSC at (a) 0, (b) 6, (c) 14, (d) 30, (e) 36 (f) 44, (g) 52 and (h) 60 minutes. The colored rings represent the logarithmic slope of the MSD, $\alpha = \frac{d\log\langle\Delta r^2(\tau)\rangle}{d\log\tau}$. This is the complete degradation profile for the data presented in Figure 2 in the main text.

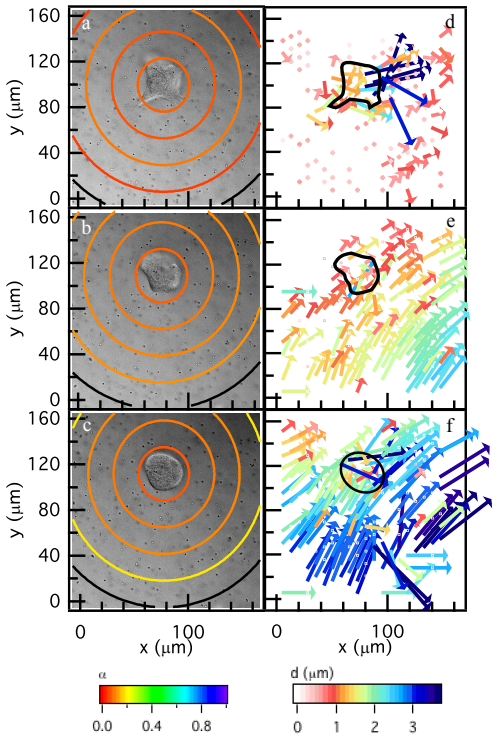

Figure S6: Spatial degradation profiles around an encapsulated hMSC prior to motility. The left column are MPT measurements and the right column are PIV measurements. MPT data are collected through time after identification of the hMSC at (a) 0, (b) 14 and (c) 26 minutes. The colored rings represent the logarithmic slope of the MSD, $\alpha = \frac{d \log \langle \Delta r^2(\tau) \rangle}{d \log \tau}$. PIV measurements are taken of brightfield images between (d) 0−6, (e) 14−20 and (f) 20−26 minutes.

Degradation profile around an MMP inhibited hMSC

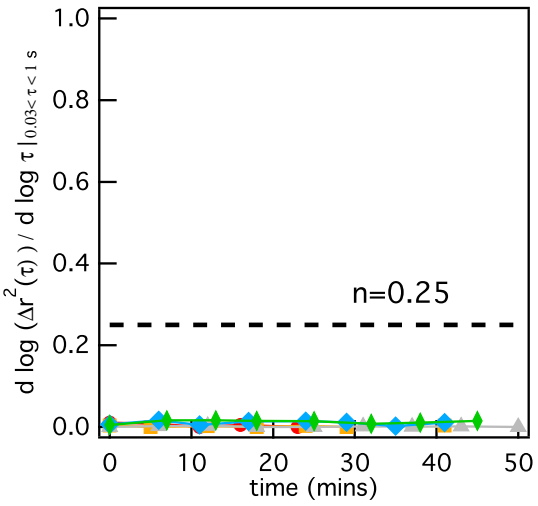

Figure S7: Measurements of the logarithmic slope of the MSD, $\alpha = \frac{d \log \langle r^2(\tau) \rangle}{d \log \tau}$, of an hMSC where MMP secretion is inhibited. The dashed line represents the critical relaxation exponent, n found in previous investigations.[1] The material is a gel when $\alpha < n$ and a sol when $\alpha > n$.

hMSC degradation in the pericellular region is also measured around cells where MMP secretion is inhibited. Data are taken over 2 days in 2 different hydrogels on $4-5$ different cells per gel. Three biological replicates are measured to ensure that the data is reproducible. Figure S7 shows changes in the state of the material around five different hMSCs encapsulated in a single hydrogel. No scaffold degradation is measured. No scaffold degradation is measured in the pericellular region across all hydrogels and all biological replicates. Additionally, all cells have a rounded morphology and are not migrating in the scaffold. The profile of degradation around an hMSC treated with the MMP inhibitor is plotted in Figure S8. Measurements shows that in the pericellular region the material is not degraded and remains in the gel phase, $\alpha \to 0$. At the time that the cell is located, $t = 0$, Figure S8a, the material is a gel and the state of the materials does not change over the measurements window, Figure S8b-c.

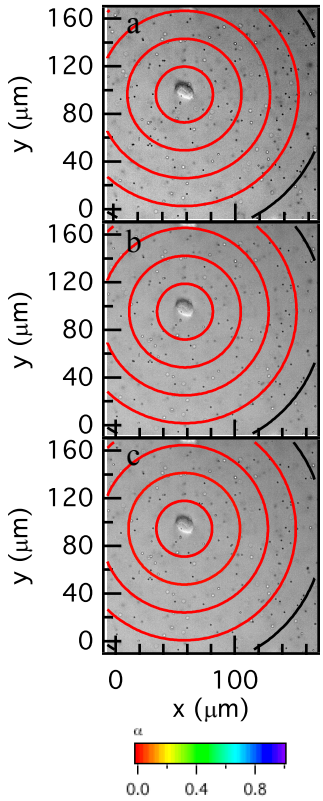

Figure S8: Spatial degradation profiles around an encapsulated hMSC after MMP inhibition. MPT data are collected through time after identification of the hMSC at (a) 0, (b)24 and (c) 44 minutes. The logarithmic slope of the MSD, $\alpha = \frac{d \log \langle \Delta r^2(\tau) \rangle}{d \log \tau}$, is identified by the color of the bounding rings and is indicative of the state of the scaffold.

Michaelis-Menten competitive inhibition reaction

The Michaelis-Menten competitive inhibition kinetic equations for MMP and TIMP binding are as following:

$$[\mathrm{E}] + [\mathrm{S}] + [\mathrm{I}] \underset{k_{-1}}{\overset{k_1}{\rightleftharpoons}} [\mathrm{ES}] + [\mathrm{I}] \xrightarrow{k_2} [\mathrm{E}] + [\mathrm{I}] + [\mathrm{D}]$$

$$[\mathrm{E}] + [\mathrm{S}] + [\mathrm{I}] \underset{k_{-3}}{\overset{k_3}{\rightleftharpoons}} [\mathrm{EI}] + [\mathrm{S}]$$

$$[\mathrm{E}] + [\mathrm{S}] \xrightarrow{k_d} [\mathrm{E}_{\mathrm{inactive}}]$$

$$[\mathrm{E}] + [\mathrm{I}] \xrightarrow{k_{di}} [\mathrm{I}_{\mathrm{inactive}}]$$

In these equations all the kinetics parameters $(k_1, k_{-1}, k_2, k_3, k_{-3}, k_d, k_{di})$ are measured previously by Olson et al. using solution experiments.[8,9] Here, E represents the enzymes or MMPs, I is the inhibitor or TIMPs, S is substrate or cross-linker, D is the product from scaffold degradation, ES is the MMP−substrate complex, EI is TIMP−substrate complex, $E_{inactive}$ is inactive MMPs, $I_{inactive}$ is inactive TIMPs and [] indicates concentration.

To derive the equation for the reaction rate, R, of MMP−TIMP unbinding we use a differential equation, which describes both the diffusion and reaction of the enzyme (MMP), E, within a shell of thickness Δr, where E is diffusing in the radial direction, r. The total effect of the two processes is accounted for by the sum of the individual rates in the process (rate of diffusion + rate of reaction of enzymes with the inhibitor, I (TIMP)).

When reaction of the enzyme, r_E, and diffusion, D, is happening in a system the following equation describes the change in enzyme concentration with time, t:

$$\frac{\partial [E]}{\partial t} = D\nabla^2 [E] + r_E \tag{1}$$

This equation for a shell with a thickness of Δr at steady state becomes:

$$D\left(\frac{\partial^2[E]}{\partial r^2}+\frac{2}{r}\frac{\partial[E]}{\partial r}\right)+r_E=0 \tag{2}$$

The reaction of the enzyme with the substrate (MMP−degradable cross-liker) is a first-order rate equation:

$$-r_E=k_{cat}[E] \tag{3}$$

where k_{cat} is the catalytic rate constant. By substituting Equation 3 into Equation 2 and dividing through D, Equation 2 becomes:

$$\frac{\partial^2[E]}{\partial r^2}+\frac{2}{r}\frac{\partial[E]}{\partial r}-\frac{k_{cat}}{D}[E]=0 \tag{4}$$

The boundary conditions used to solve this equation are:

$$1)\ [E]=[E_0]\ \text{at}\ r=r_0$$

$$2)\ [E]=0\ \text{at}\ r=\infty$$

where $[E_0]$ is the initial enzyme concentration and r_0 is the radius of the cell. Solving Equation 4, we write the equation in dimensionless form using the following dimensionless variables:

$$\phi=r\sqrt{\tfrac{k_{cat}}{D}}$$

$$\varphi=\tfrac{[E]}{[E_0]}$$

$$\lambda=\tfrac{r}{r_0}$$

where ϕ is the Thiele modulus. Substituting dimensionless variables into Equation 4, this equation becomes:

$$\frac{\partial^2\varphi}{\partial\lambda^2}+\frac{2}{\lambda}\frac{\partial\varphi}{\partial\lambda}-\phi^2\varphi=0 \tag{5}$$

The dimensionless boundary conditions are:

$$1)\ \varphi=1\ \text{at}\ \lambda=1$$

$$2)\ \varphi=0\ \text{at}\ \lambda=0$$

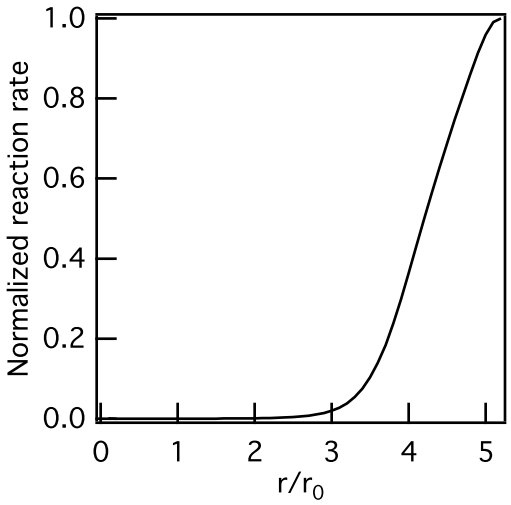

Figure S9: Reaction rate of MMP−2 unbinding from TIMP−2 as a function of normalized distance measured from the cell center calculated from Michaelis-Menten competitive inhibition kinetics.

The dimensionless enzyme concentration distribution, $\frac{[E]}{[E_0]}$ is:

$$\frac{[E]}{[E_0]} = \frac{e^{\left(-\phi\left(\frac{r}{r_0}-1\right)\right)}}{\frac{r}{r_0}} \tag{6}$$

By solving Equation 5 the solution for the rate of reaction, R, for MMP−TIMP unbinding is:

$$R = [E_0] \times \frac{e^{\left(-\phi\left(\frac{r}{r_0}-1\right)\right)}}{\frac{r}{r_0}} \tag{7}$$

where $[E_0] = [E] + [ES] + [EI]$. $[E_0]$ is determined from Michaelis-Menton competitive inhibition kinetics by assuming the system is at steady-state and the substrate and inhibitor concentrations do not change significantly. The total enzyme concentration is:

$$[E_0] = \left(\frac{\frac{k_{off}}{k_{on}}[I_0][S_0][E]}{1 + \left(\frac{k_{off}}{k_{on}} + \frac{k_{des}}{k_{ads}}\right)[E] + \frac{k_{off}}{k_{on}}\frac{k_{des}}{k_{ads}}[E]^2} \right) \tag{8}$$

Therefore, the reaction rate of MMP−TIMP unbinding, R, as a function of distance from

the cell, r, is:

$$R = \left(\frac{\frac{k_{off}}{k_{on}}[I_0][S_0][E]}{1 + \left(\frac{k_{off}}{k_{on}} + \frac{k_{des}}{k_{ads}}\right)[E] + \frac{k_{off}}{k_{on}}\frac{k_{des}}{k_{ads}}[E]^2} \right) \times \frac{e^{\left(-\phi\left(\frac{r}{r_0}-1\right)\right)}}{\frac{r}{r_0}} \tag{9}$$

where k_{on} and k_{off} are the rate of TIMP binding and unbinding to MMPs, $[S_0]$ and $[I_0]$ are the initial substrate and inhibitor concentrations, k_{ads} and k_{des} are the rates of adsorption and desorption and are tabulated in Olson et al.[9]

Figure S9 is the rate (Equation 9) of MMP−2−TIMP−2 unbinding. The maximum MMP activity occurs at $r = 52\mu m$. The distance from the cell center is similar to the value calculated for MMP−2 activity inhibited by TIMP−1 (Figure 4 in the main text).

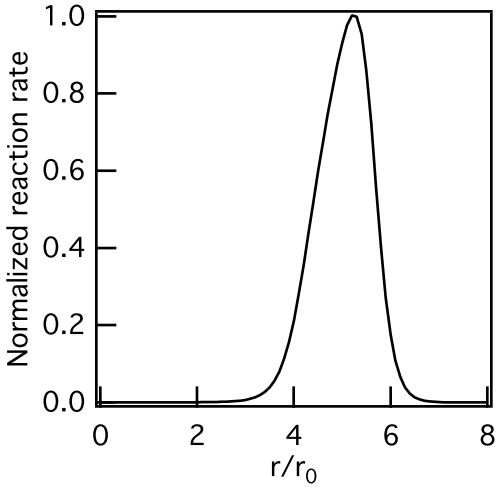

Figure S10: Reaction rate of MMP−2 unbinding from TIMP−1 as a function of normalized distance measured from the cell center calculated from Michaelis-Menten competitive inhibition equations.

Figure S10 shows the complete normalized reaction rate for MMP−2−TIMP−1 unbinding (this plot is cut in the main text at the maximum rate). This figure indicates that the maximum unbinding rate happens at five times the initial cell radius (50 μm) and then decrease significantly at $r = 70$ μm. This model is predicting activity due to MMP−TIMP unbinding. Therefore, in the area past the maximum reaction rate (over 70 μm from the cell center) the model predicts a decrease in MMP−TIMP unbinding, which is expected since

the maximum unbinding rate has already been achieved.

References

(1) Schultz, K. M.; Anseth, K. S. Monitoring degradation of matrix metalloproteinases-cleavable PEG hydrogels via multiple particle tracking microrheology. *Soft Matter* **2013**, *9*, 1570–1579, DOI: 10.1039/c2sm27303a.

(2) Fairbanks, B. D.; Schwartz, M. P.; Bowman, C. N.; Anseth, K. S. Photoinitiated polymerization of PEG-diacrylate with lithium phenyl-2,4,6- trimethylbenzoylphosphinate: polymerization rate and cytocompatibility. *Biomaterials* **2009**, *30*, 6702–6707, DOI:10.1016/j.biomaterials.2009.08.055.

(3) Kovacs, M.; Toth, J.; Hetenyi, C.; Malnasi-Csizmadia, A.; Sellers, J. R. Mechanism of Blebbistatin Inhibition of Myosin II. *Biological Chemistry* **2004**, *279*, 35557–35563, DOI: 10.1074/jbc.M405319200.

(4) Schultz, K. M.; Kyburz, K. A.; Anseth, K. S. Measuring dynamic cell-material interactions and remodeling during 3D human mesenchymal stem cell migration in hydrogels. *Proceedings of the National Academy of Sciences* **2015**, *112*, E3757–E3764, DOI:10.1073/pnas.1511304112.

(5) Crocker, J. C.; Grier, D. G. Methods of Digital Video Microscopy for Colloidal Studies. *Journal of colloid and interface science* **1996**, *179*, 298–310, DOI:10.1006/jcis.1996.0217.

(6) Mason, T. G.; Weitz, D. A. Optical Measurements of Frequency-Dependent Linear Viscoelastic Moduli of Complex Fluids. *Physcical review letter* **1995**, *74*, DOI: 10.1103/PhysRevLett.74.1250.

(7) Savin, T.; Doyle, P. S. Static and dynamic errors in particle tracking microrheology. *Biophys. J.* **2005**, *88*, 623–638, DOI: 10.1529/biophysj.104.042457.

(8) Patterson, J.; Hubbell, J. Enhanced proteolytic degradation of molecularly engineered PEG hydrogels in response to MMP-1 and MMP-2. *Biomaterials* **2010**, *31*, 7836–7845, DOI: 10.1016/j.biomaterials.2010.06.061.

(9) Olson, M. W.; Gervasi, D. C.; Mobashery, S.; Fridman, R. Kinetic Analysis of the Binding of Human Matrix Metalloproteinase-2 and -9 to Tissue Inhibitor of Metalloproteinase (TIMP)-1 and TIMP-2. *Biological Chemistry* **1997**, *272*, 29975–29983, DOI: 10.1074/jbc.272.47.29975.